RSC Advances

PAPER

View Article Online
View Journal | View Issue

Cite this: *RSC Adv.*, 2020, **10**, 3675

Synthesis of new oxadiazol-phthalazinone derivatives with anti-proliferative activity; molecular docking, pro-apoptotic, and enzyme inhibition profile†

Mohamed H. Hekal,[a] Abeer M. El-Naggar,*[a] Fatma S. M. Abu El-Azm[a] and Wael M. El-Sayed*[b]

Background and aim: The current study reports the synthesis and biological evaluation of two novel series of 4-(5-mercapto-1,3,4-oxadiazol-2-yl)phthalazin-1(2*H*)-one derivatives. *Methods*: The synthetic reactions were carried out under both conventional and ultrasonic irradiation conditions. The anti-proliferative activity of the newly synthesized compounds against two human epithelial cell lines; liver (HepG2) and breast (MCF-7) in addition to normal fibroblasts (WI-38) was investigated. In addition to molecular docking studies, the possible mechanism(s) of action were also explored. *Results*: In general, an improvement in synthetic rates and yields was observed when reactions were carried out under sonication compared with classical conditions. The structures of the products were established based on analytical and spectral data. Derivatives **2e** and **7d**, in addition to compound **1**, had significant and selective anti-proliferative activity against liver and breast cancer cell lines without harming normal fibroblasts. These derivatives arrested the cell cycle progression and/or induced apoptosis. This has been manifested by the elevation in the expression of p53 and caspase 3, down-regulation of cdk1, and a reduction in the concentrations of MAPK and Topo II at submicromolar concentrations. The latter results confirmed the molecular docking study. *Conclusions*: Compound **1** had the best profile on the gene and protein levels (arresting cell cycle and inducing apoptosis). The ability of compounds **1** and **2e** to inhibit both MAPK and Topo II nominates these derivatives as potential candidates for further anticancer and antitumor studies.

Received 1st November 2019
Accepted 15th January 2020

DOI: 10.1039/c9ra09016a

rsc.li/rsc-advances

1. Introduction

Phthalazin-1(2*H*)-ones and (alkyl or aryl)thio-1,3,4-oxadiazoles serve as important building blocks for biologically active molecules. The structures of these two important biologically active pharmacophore component systems are shown in Fig. 1.

The phthalazin-1(2*H*)-one nucleus has emerged as a promising and attractive scaffold in the preparation of promising antitumor agents. For example, phthalazin-1,4-diones have been reported as potent type II IMP dehydrogenase inhibitors[1] and as active anti-proliferative agents against various human and murine tumor cells,[2,3] particularly hepatocellular carcinoma.[4] In addition, a series of 4-substituted-2*H*-phthalazin-1-ones has been studied as potent orally bioavailable poly ADP ribose polymerase (PARP) inhibitors.[5–7] Olaparib (**1**), MRU-868 (**2**) and KU0058958 (**3**) are the most interesting PARP inhibitors based on the 4-substituted-2*H*-phthalazin-1-one scaffold (Fig. 2).

The second pharmacophore component, 1,3,4-oxadiazoles, is an important category of heterocyclic compounds with a wide range of biological activities such as antimicrobial,[8] antiviral,[9] fungicidal,[10] antineoplastic,[11] inhibition of tyrosinase,[12] anticancer[13–16] and inhibition of cathepsin K.[17] They are also useful intermediates in organic synthesis[18] and they are widely utilized

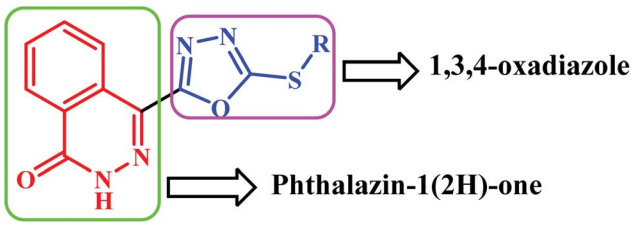

Fig. 1 Phthalazinone-oxadiazoles scaffold.

[a]*Department of Chemistry, Faculty of Science, Ain Shams University, Abbassia 11566, Cairo, Egypt. E-mail: elsayedam@sci.asu.edu.eg*

[b]*Department of Zoology, Faculty of Science, Ain Shams University, Abbassia 11566, Cairo, Egypt. E-mail: waelelhalawany@hotmail.com; wael_farag@sci.asu.edu.eg; Fax: +202/2684-2123; Tel: +202/2482-1633*

† Electronic supplementary information (ESI) available. See DOI: 10.1039/c9ra09016a

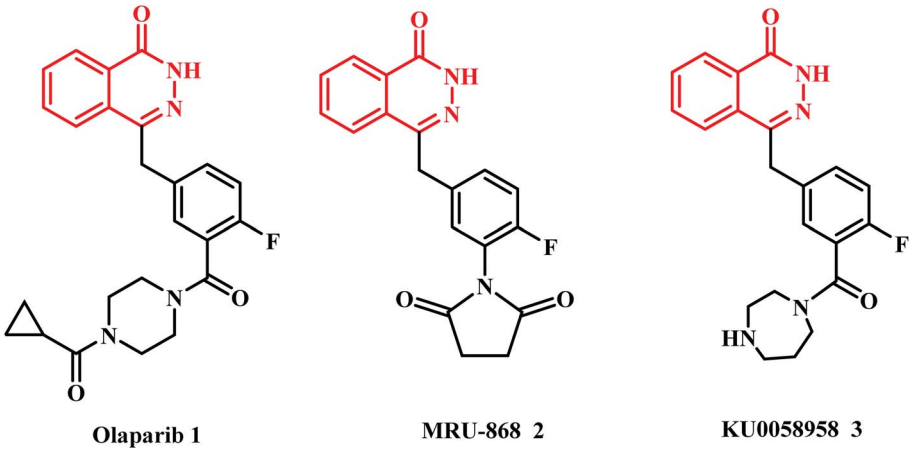

Fig. 2 Structure of the lead anticancer phthalazin-1(2*H*)-one derivatives **1–3**.

as electron transporting and hole-blocking materials.[19] Further, 1,3,4-oxadiazole heterocycles are recognized as bioisosteres of esters and amides that can contribute interesting pharmacokinetic properties due to the presence of N–C=O linkage in the oxadiazole nucleus, which increases lipophilicity and affects the ability of the drugs to reach molecular targets by transmembrane diffusion. These molecules are often utilized as

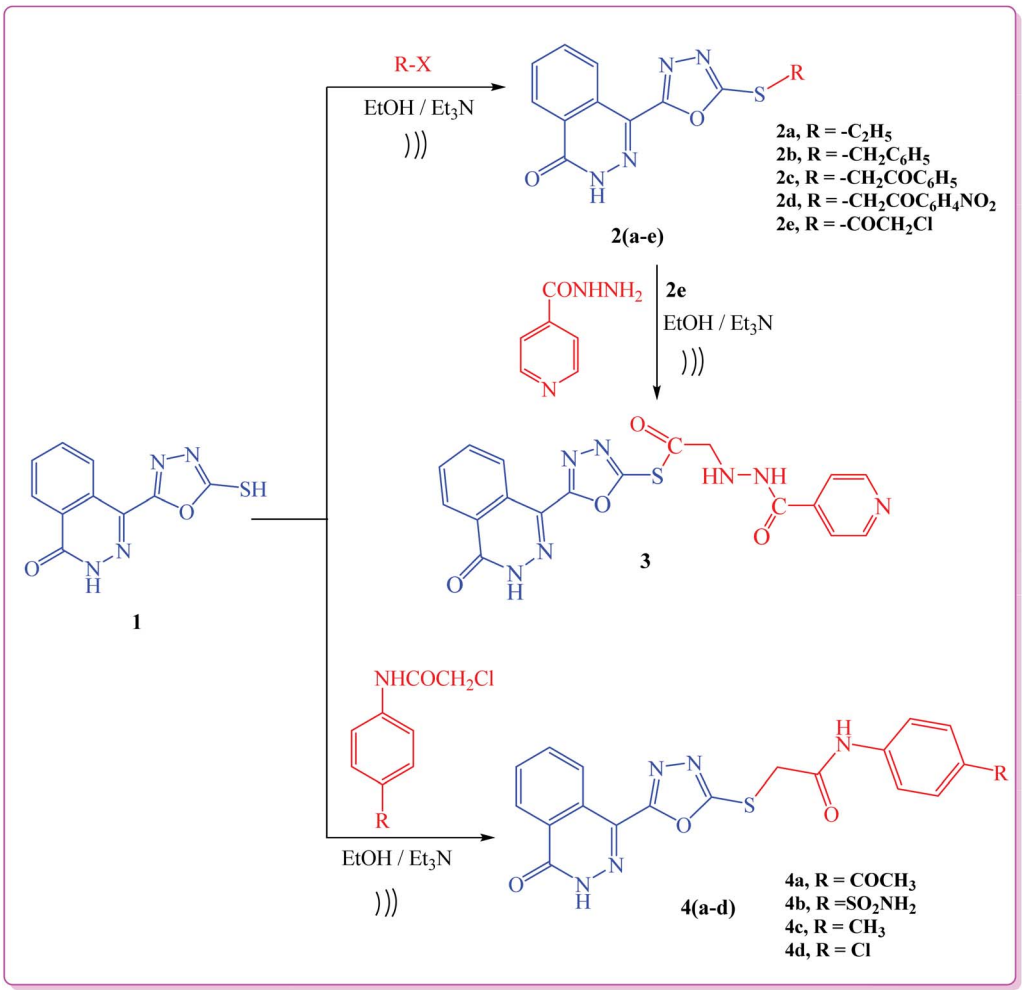

Scheme 1 General procedure for synthesis of target compounds (**2a–e**, **3**, **4a–d**).

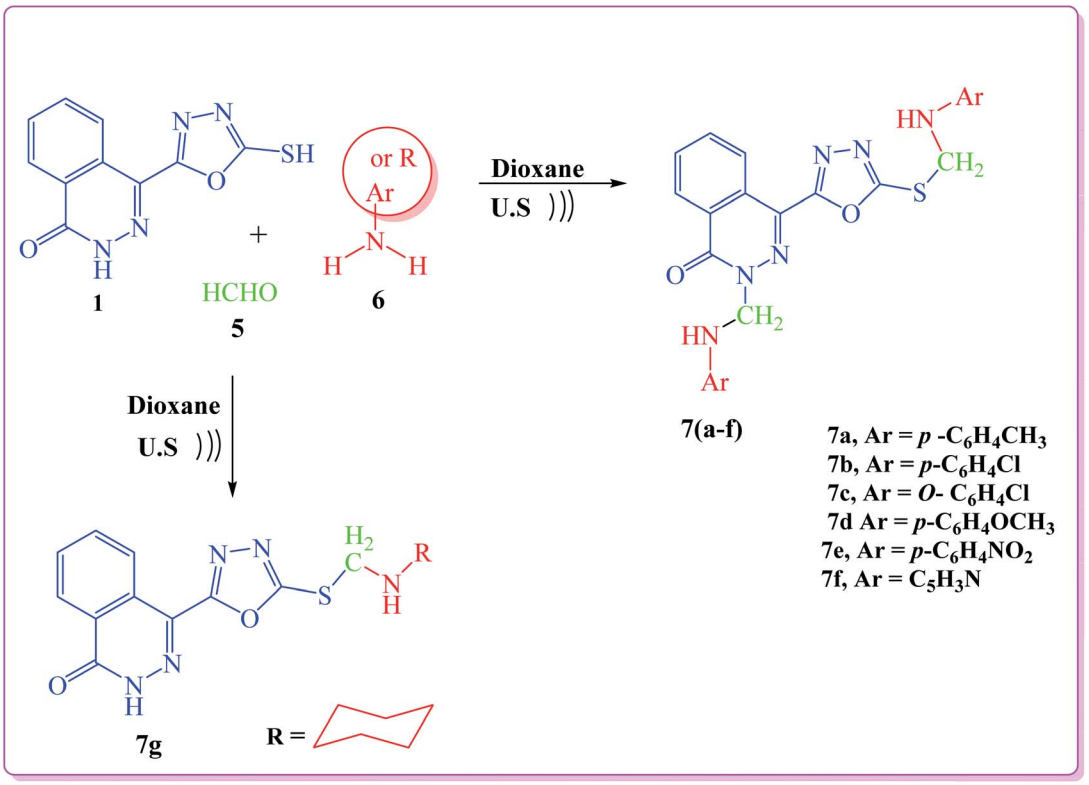

Scheme 2 General procedure for synthesis of target compounds (**7a–g**).

Table 1 Comparison between conventional and ultrasonic irradiation (US) methods for synthesis of substituted 4-(1,3,4-oxadiazol-2-yl) phthalazin-1(2*H*)-ones at room temperature

		Ultrasonic irradiation		Conventional	
Entry	Comp. no.	Time (min)	Yield (%)	Time (min)	Yield (%)
1	**2a**	5	92	55	70
2	**2b**	7	90	65	71
3	**2c**	5	87	65	67
4	**2d**	5	85	50	62
5	**2e**	4	86	50	66
6	**3**	8	93	55	75
7	**4a**	10	92	75	73
8	**4b**	9	94	70	77
9	**4c**	7	90	65	74
10	**4d**	10	91	75	70
11	**7a**	5	94	75	68
12	**7b**	7	93	80	76
13	**7c**	7	90	72	74
14	**7d**	5	91	80	67
15	**7e**	7	92	83	77
16	**7f**	8	88	71	69
17	**7g**	10	95	80	75

pharmacophores due to their ability to bind target proteins through hydrogen bond formation.[20]

The biological activities of these pharmacophores, phthalazin-1(2*H*)-one and 1,3,4-oxadiazole, led us to design and synthesize novel lead compounds containing the two pharmacophores in a single molecule with the goal of increasing pharmacological activities. The synthetic reactions were carried out under both conventional and ultrasonic irradiation conditions. Ultrasound has been increasingly used in organic synthesis in recent years. A large number of organic reactions can be carried out in higher yield, shorter reaction time and milder conditions under ultrasonic irradiation.[21,22] The phenomenon observed is known as "acoustic cavitation" and generates high temperatures and pressures in localized zones of the liquid, creating rate acceleration in many chemical reactions.[23] In addition, multicomponent reactions have received considerable attention, since they show good atom economy; they are highly convergent and require minimal time and effort to obtain complex molecules.[24]

A series of 18 new compounds was synthesized and examined for anti-proliferative activity against two human epithelial breast and liver cancer cell lines, as well as normal fibroblasts. The lead compounds showing significant anti-proliferative activity were further investigated on the expression of crucial genes involved in cell cycle progression and apoptosis. Finally, these lead compounds were evaluated as inhibitors of key enzymes involved in cell cycle and cellular proliferation: p38 mitogen-activated protein kinase (MAPK) and topoisomerase II. The ability of molecular docking to predict the inhibitory effects of the lead derivatives against topoisomerase II and serine/threonine-protein kinase (PIM1) was also examined. The parent compound **1** was docked against these two key enzymes because the two pharmacophores used in the current study were separately demonstrated to possess significant anticancer activity.

Table 2 Influence of the oxadiazol-phthalazinone derivatives on the viability of HepG2, MCF7 and WI-38 cells

	IC_{50} (μM)		
Cpd	HepG2	MCF7	WI-38
DOX	4.5 ± 0.3	4.2 ± 0.2	6.7 ± 0.5
1	4.5 ± 1.1	4.9 ± 0.8	74.9 ± 2.4
2a	61.3 ± 4.2	55.8 ± 4.0	39.1 ± 2.9
2b	58.9 ± 4.0	68.2 ± 4.4	42.2 ± 3.3
2c	66.1 ± 4.5	57.3 ± 4.2	23.5 ± 1.9
2d	>100	>100	29.5 ± 2.2
2e	6.9 ± 1.3	5.0 ± 1.5	72.4 ± 4.8
3	38.4 ± 3.5	40.0 ± 3.6	44.6 ± 4.2
4a	72.6 ± 4.8	76.2 ± 4.7	35.4 ± 2.7
4b	83.9 ± 5.2	>100	32.9 ± 2.5
4c	28.1 ± 2.9	36.3 ± 3.2	66.0 ± 4.7
4d	53.9 ± 3.8	49.5 ± 3.9	45.7 ± 3.5
7a	23.5 ± 2.8	26.2 ± 2.5	62.8 ± 4.5
7b	33.3 ± 3.4	31.3 ± 2.8	51.4 ± 4.1
7c	17.2 ± 1.9	15.4 ± 1.2	23.2 ± 1.2
7d	6.3 ± 0.7	5.5 ± 0.4	68.6 ± 2.1
7e	7.0 ± 1.5	8.4 ± 0.9	21.6 ± 1.8
7f	21.8 ± 2.3	20.8 ± 1.9	58.1 ± 4.3
7g	42.9 ± 3.7	45.5 ± 3.8	49.2 ± 3.9

Table 3 Effect of oxadiazol-phthalazinone derivatives on the expression of p53, cdk1, caspase 3 and txnrd1 in HepG2 after 8 h incubation

	Fold induction from untreated cells			
Treatment	p53	Cdk1	Caspase 3	Txnrd1
DOX	2.15 ± 0.41[a]	0.25 ± 0.06[a]	4.10 ± 0.35[a]	0.44 ± 0.11[a]
1	3.83 ± 0.11[a]	0.22 ± 0.03[a]	3.10 ± 0.21[a]	0.67 ± 0.03
2e	1.63 ± 0.18	1.04 ± 0.25	0.98 ± 0.12	0.93 ± 0.09
7c	1.37 ± 0.05	1.21 ± 0.14	1.19 ± 0.13	0.96 ± 0.14
7d	2.16 ± 0.12[a]	0.98 ± 0.11	1.96 ± 0.09[a]	1.02 ± 0.16
7e	2.02 ± 0.08[a]	1.04 ± 0.09	2.22 ± 0.14[a]	1.11 ± 0.10

[a] Significant difference ($p < 0.05$) as compared to untreated cells. The data are expressed as mean ± SEM for two independent experiments.

2. Results and discussion

2.1. Chemistry

As a part of our interest in the synthesis of a wide range of heterocyclic systems with biological applications,[25–29] and in a continuation of using green chemistry tools in heterocyclic synthesis,[30–33] our current research is concerned with the utility of 4-(5-mercapto-1,3,4-oxadiazol-2-yl)phthalazin-1(2*H*)-one (**1**)[34] in the synthesis of new substituted 4-(1,3,4-oxadiazol-2-yl) phthalazin-1(2*H*)-one derivatives under both conventional and ultrasonic irradiation conditions.

In this study, we report an efficient method for the synthesis of a series of 4-(1,3,4-oxadiazol-2-yl)phthalazin-1(2*H*)-one derivatives *via* alkylation of compound **1** with the appropriate alkyl and acyl halides namely, ethyl iodide, benzyl chloride, phenacyl bromide, *m*-nitrophenacyl bromide and chloroacetyl chloride in ethanol and in the presence of catalytic amount of triethylamine to afford the target compounds **2a–e** (Scheme 1). The structures of compounds **2a–e** were elucidated from their spectroscopic data. Their IR spectra exhibited absorption bands corresponding to NH group in the range 3247–3158 cm^{-1} as well as bands for C=O group at 1657–1688 cm^{-1}.

When compound **2e** was allowed to react with isonicotinohydrazide, it yielded the hydrazide derivative **3** (Scheme 1). Finally, reaction of compound **1** with the appropriate 2-chloro-*N*-substituted phenylacetamide derivatives afforded 4-(1,3,4-oxadiazol-2-yl)phthalazin-1(2*H*)-one derivatives **4a–d** (Scheme 1). The ^{1}H NMR (DMSO) spectra of compounds **4a–d** revealed the presence of broad signals for (NH) protons at 10.77–13.38 ppm, and a singlet signal characteristic for SCH_2 protons at 4.45 ppm.

In addition, a Mannich reaction was performed through a one-pot three-component reaction. An ultrasound-assisted reaction between 4-(5-mercapto-1,3,4-oxadiazol-2-yl)phthalazin-1(2*H*)-one (**1**), formaldehyde (**5**), and primary amines (**6**) namely, *p*-toluidine, *p*-chloroaniline, *o*-chloroaniline, *p*-anisidine, *p*-nitroaniline, 3-aminopyridine and cyclohexyl amine, afforded 4-(1,3,4-oxadiazol-2-yl)phthalazin-1(2*H*)-one derivatives (**7a–g**), respectively, in good yield (Scheme 2).

The IR spectra of the products lacked the SH absorption peak and showed the C=O peak at 1666–1691 cm^{-1}. The ^{1}H NMR spectra of the products (**7a–g**) showed that the methylene groups (SCH_2N and NCH_2N) attached to asymmetric nitrogen are magnetically non-equivalent (diastereotopic proton) and they appear as dd (quartet) signals in the range of δ 5.39–5.56 and 5.50–5.99, respectively. The NH proton appears as multiplet in the range 12.99–13.45 due to the quadrapole moment of nitrogen atom. The ^{1}H NMR spectra of compound **7f** showed two multiplet signals at 4.57–5.08 and 5.12–5.49 (high field) attributed to the two NH groups (SCH_2NH and NCH_2NH), respectively. This is due to the presence of NH group in position three of pyridine moiety.

The methodology presented is easy, atomically economical, fast, and environmentally benign. The synthesis of the target compounds was carried out as outlined in Schemes 1 and 2. It was observed that the ultrasonic approach proved to be extremely fast providing good to excellent yields (85–94%) as compared with the conventional method (62–77%). The results are summarized in Table 1. The structures of all newly prepared compounds were confirmed by spectral and elemental analyses, which were in full agreement with the proposed structures.

2.2. Biology

2.2.1 *In vitro* anti-proliferative activity. The *in vitro* anti-proliferative activity of the 18 novel oxadiazol-phthalazinone derivatives was assessed against human liver (HepG2) and breast (MCF7) cancer cell lines in addition to normal fibroblasts (WI-38) and compared to the activity of doxorubicin (Table 2). The data showed that doxorubicin had an IC_{50} of ~4–7 μM against all cells investigated with no differentiation between cancer and normal cells. The novel oxadiazol-phthalazinone derivatives (**1**, **2e**, **7c**, **7d** and **7e**) showed promising anti-proliferative activity against cancer cell lines with IC_{50}s of 5.5–

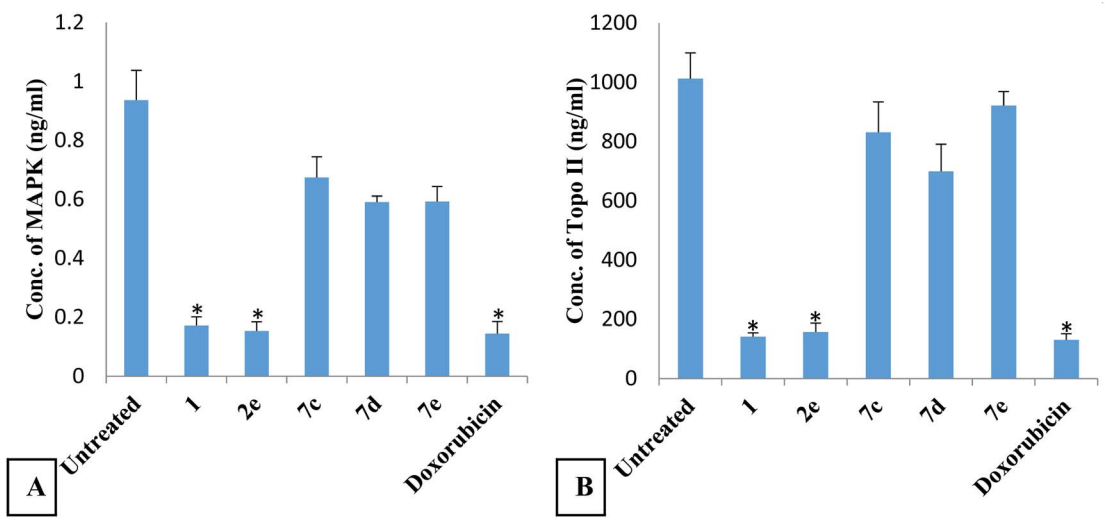

Fig. 3 The effect of the novel oxadiazol-phthalazinone derivatives on MAPK (A) and topoisomerase II (Topo II) (B) concentrations in HepG2 cells. Each compound has been assigned three wells and the experiment was performed twice. Data are expressed as mean ± SEM. * Significant inhibition compared to untreated cells. There was no significant difference between derivatives **1** and **2e** and doxorubicin.

15 μM. Only three derivatives (**1**, **2e** and **7d**) were safe to the normal fibroblasts with IC_{50}s of ~70–75 μM. The other two derivatives (**7c** and **7e**) showed some toxicity against the fibroblasts at ~23 and 22 μM, respectively; a concentration four times that of doxorubicin. This indicates that derivatives **1**, **2e** and **7d** have selectivity against cancer cell lines and, therefore, these derivatives were chosen for more focused mechanistic studies.

The viability of cells was measured after 48 h of incubation with 5 different concentrations (three wells per every concentration) of the investigated compounds by MTT assay. The IC_{50} was determined from the dose–response curves as the mean of two parallel experiments. Doxorubicin (Dox) was used as a positive control. The data are expressed as mean ± SEM.

2.2.2 qRT-PCR assessment of the expression of p53, cdk1, caspase-3, and txnrd1. To investigate the molecular mechanism(s) through which these active derivatives exerted their anti-proliferative activity, the expression of some key genes involved in cell cycle progression and apoptosis was investigated (Table 3). The HepG2 cells were treated with the derivatives (**1**, **2e** and **7c–7e**) that showed promising anti-proliferative activity, in addition to doxorubicin, and the expression of four key genes in the cell cycle (p53, caspase 3, cdk1, and txnrd1) was assessed. Doxorubicin caused significant 2-fold and 4-fold elevations in p53 and effector caspase 3, respectively. Similar effects were previously reported for doxorubicin.[35] It also caused ~75% inhibition in cdk1 expression in agreement with previous reports.[36] Derivatives **7d** and **7e** caused a 2-fold increase in both p53 and caspase 3 but were devoid of any significant effect on

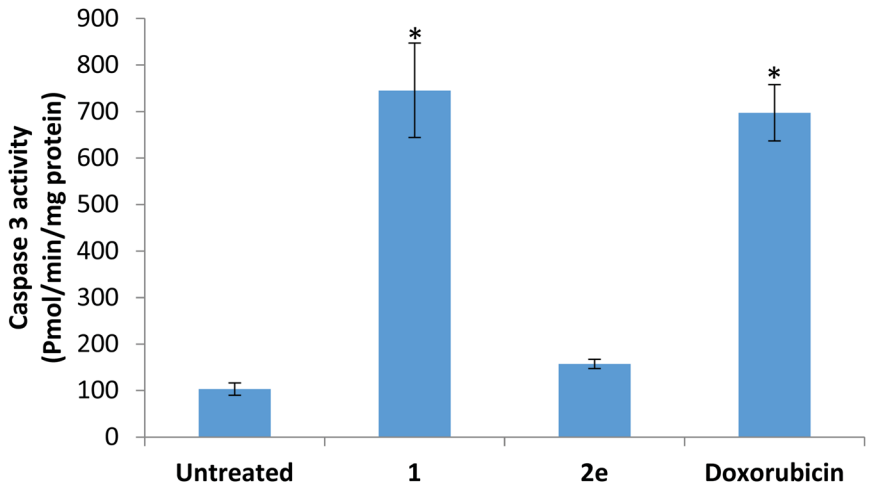

Fig. 4 The effect of derivatives **1** and **2e** on cleaved caspase 3 activity in HepG2 cells. Data are expressed as mean ± SEM. * Significant inhibition compared to untreated cells.

Table 4 The docking binding free energies of the derivatives **1** and **2e** with PIM1 and topoisomerase II forming hydrogen bonding and cationic-π interactions

	PIM1			Topoisomerase II		
Comp. no.	ΔG kcal mol^{-1}	No. of H bonds	No. of π bonds	ΔG kcal mol^{-1}	No. of H bonds	No. of π bonds
1	−5.69	2 (Asp168, Met109)	1 (Ile84)	−6.06	2 (Asp78, Asn51)	2 (Met83 and Met83)
2e	−5.93	3 (Thr106, Met109 and Lys53)	(Val38, Leu108)	−6.04	Ser124	—
Ligand	−6.61	3 (Asp112, Thr106 and Met109)	—	−6.44	3 (Asp78, Arg140 and Arg 140)	—

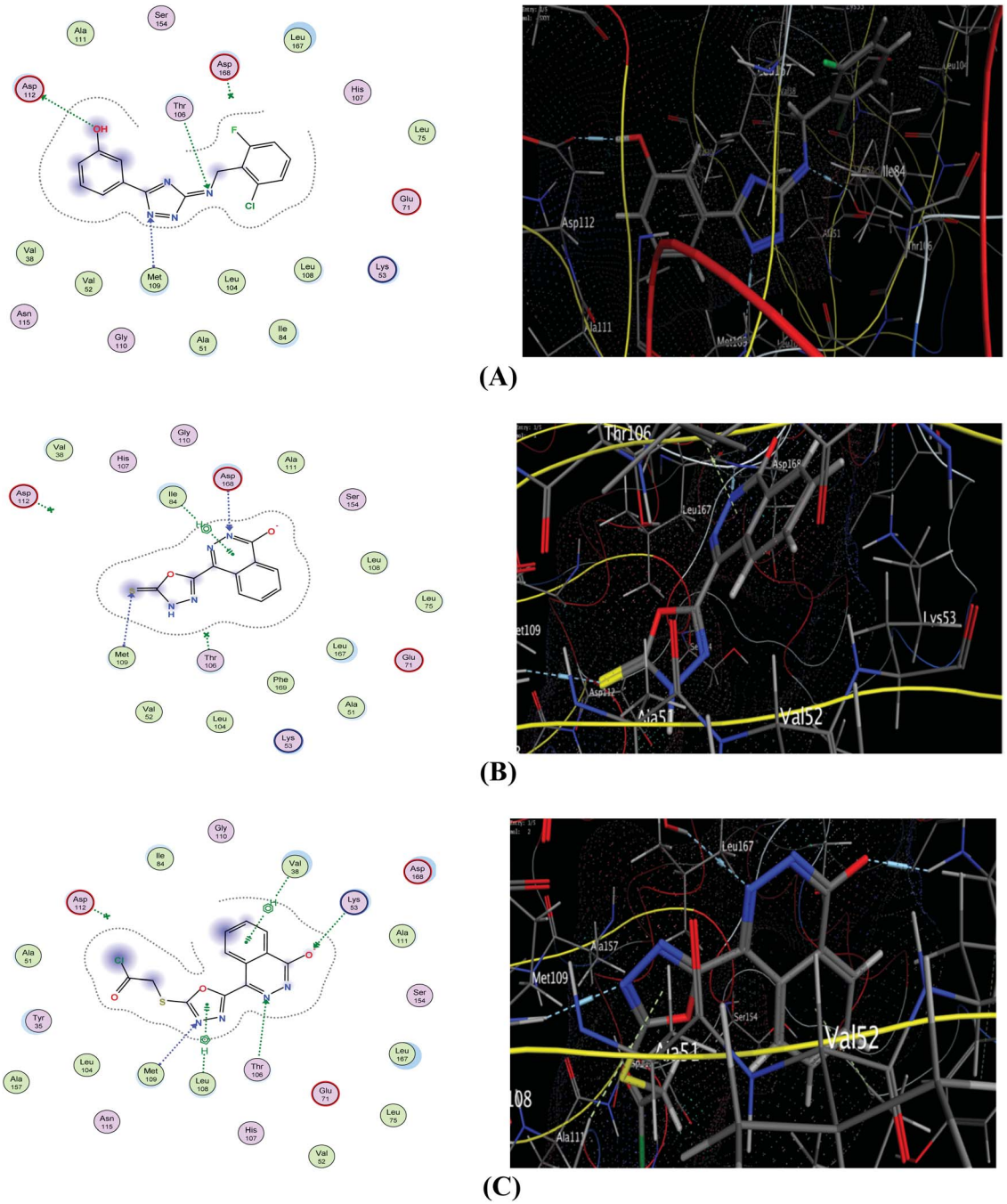

Fig. 5 2D (left) and 3D (right) diagrams of binding interactions of ligand (A), compound **1** (B), and derivative **2e** (C) with PIM1.

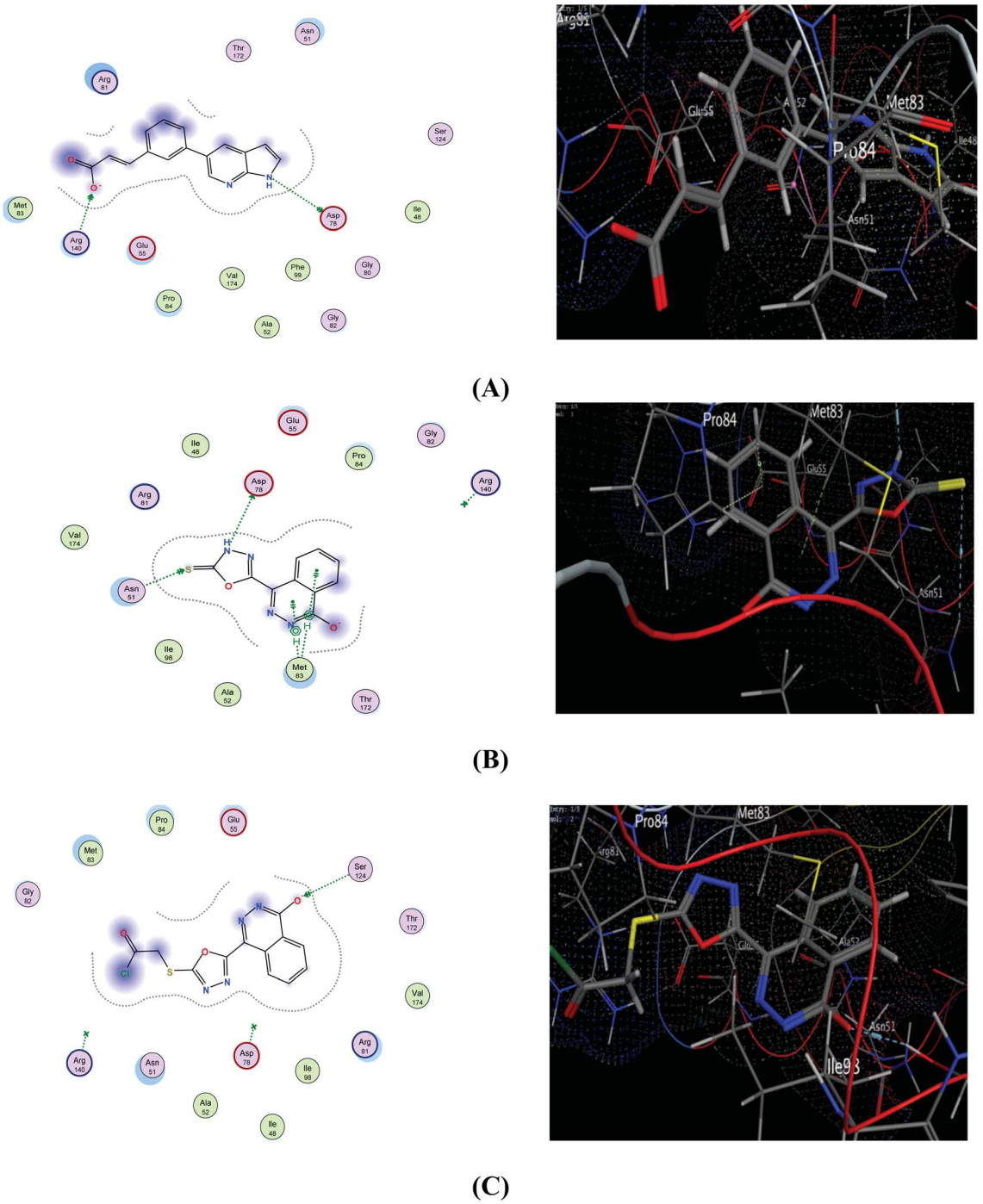

Fig. 6 2D (left) and 3D (right) diagrams of binding interactions of ligand (A), compound **1** (B), and derivative **2e** (C) with Topo II.

Table 5 Sequences of primers used for the Real-time PCR analysis

Gene	Forward primer	Reverse primer
p53	CTGCCCTCAACAAGATGTTTTG	CTATCTGAGCAGCGCTCATGG
Cdk1	CCGAAATCTGCCAGTTTGAT	CTGGCCAGTTCATGGATTCT
Caspase-3	TTAATAAAGGTATCCATGGAGAACACT	TAGTGATAAAAATAGAGTTCTTTTGTGAG
Txnrd1	GTTACTTGGGCATCCCTGGTGA	CGCACTCCAAAGCGACATAGGA
GAPDH	TCAAGAAGGTGGTGAAGCAG	AGGTGGAAGAATGGGAGTTG

cdk1. Compound **1** up-regulated the expression of p53 and caspase 3 by ~4- and 3-fold, respectively. It also was the only derivative that inhibited the expression of cdk1 by ~78%. Doxorubicin down-regulated the expression of thioredoxin reductase 1 (txnrd1) by 56%; none of the investigated derivatives significantly affected the expression of this enzyme. Doxorubicin was previously reported to elevate the expression and activity of txnrd1.[37] Derivatives **7c** (the most toxic derivative to the normal fibroblasts) had no significant effect on any of the genes investigated in the current study.

p53 is a tumor suppressor gene and widely known as the guardian of the genome. It is mutated in more than 50% of human cancer types.[38] It plays a central role in the regulation of cell cycle progression, apoptosis, and DNA stability. DNA damage signals the increase in p53 expression, which arrests the cell cycle at the G1/S checkpoint, activates DNA repair mechanisms, and if the damage is severe, p53 initiates apoptosis.[39] The elevation in p53 in the current study could be responsible for the parallel elevation in the expression of caspase 3. Caspase 3 is the main execution member responsible for apoptosis induced by both extrinsic and intrinsic pathways.[40] However, the elevation in the expression level of caspase 3 should result in the elevation of active cleaved enzyme to indicate the occurrence of apoptosis. The ability of the cell to progress to S phase depends on cdk1.[41] The downregulation of cdk1 by doxorubicin and compound **1**, along with the elevation in p53 expression, suggests cell cycle arrest. Derivative **1** was the only investigated compound that downregulated the expression of cdk1. This could be attributed to the 4-fold elevation in p53 *versus* the 2-fold increase by derivatives **7d** and **7e**. However, this assumption of the p53 threshold elevation is not supported by the doxorubicin results. Doxorubicin also caused only a 2-fold increase in p53 and, at the same time, downregulated cdk1 expression. Therefore, we believe that derivative **1** directly acted on the cdk1 gene in addition to its effects on p53, but this assumption needs further investigation. The last gene investigated, txnrd1, is the only known enzyme that reduces thioredoxin.[42] Thioredoxin in turn reduces several proteins and forms the disulfide bonds crucial for the activity of these proteins. Thioredoxin and txnrd1 are essential for cell growth and survival. Therefore, this enzyme is upregulated in many types of cancer.[43] Inhibition of txnrd1 leads to cell death.[44] Unfortunately, none of oxadiazol-phthalazinone derivatives significantly inhibited the expression of this enzyme. The 33% inhibition by compound **1** did not achieve statistical significance.

2.2.3 Inhibitory activity of novel oxadiazol-phthalazinone derivatives on p38 mitogen-activated protein kinase (MAPK) and topoisomerase II (Topo II). The HepG2 cells were treated with the active five derivatives (**1**, **2e**, and **7c–7e**) at the IC_{50} concentrations reported in Table 2 for 8 hours. A standard curve was created using a four parameter logistic curve-fit. Derivatives **7c–e** caused no significant reduction in MAPK concentration. These derivatives reduced the enzyme concentration by 28–37% (Fig. 3A). Derivatives **1** and **2e** decreased the enzyme concentration by 84 and 82%, respectively as compared to untreated cells. Doxorubicin caused a 85% reduction in the MAPK concentration. MAP kinases are involved in many cellular processes including proliferation, gene expression, and apoptosis. Therefore, these enzymes are targets for many antitumor chemotherapeutic agents. Sorafenib, a successful anticancer agent, is a MAPK inhibitor.[45] In a similar scenario, derivatives **1** and **2e** decreased the Topo II concentration by 84 and 86%, respectively, and similar to the 87% decrease caused by doxorubicin (Fig. 3B). Derivatives **7c–e** caused 9–31% decrease in the enzyme concentration. The 31% reduction in enzyme concentration caused by derivative **7d** did not achieve a statistical significance ($p = 0.058$). Topo II prevents DNA tangling by inducing double stranded breaks and is an essential enzyme for DNA replication and cell proliferation.[46] Inhibitors of Topo II have been extensively examined as antineoplastic agents.[47] Initially in the current study, doxorubicin was selected as a reference drug since it is listed by the WHO as an essential effective and safe medicine in the health system. Later, it has been used for comparison since the main action of doxorubicin is to slow or stop the growth of cancer cells by arresting the cell cycle and blocking Topo II, which is the proposed main target of the novel derivatives described in this study.

2.2.4 Effect of compound 1 and derivative 2e on the cleaved caspase 3 activity in HepG2. Because a linear correlation between gene expression and protein expression does not always exist and because caspase 3 exists as inactive procaspase 3, measuring the cleaved caspase 3 activity is considered the most accurate way to examine the effect of the most active compounds from the previous investigations (**1** and **2e**) on caspase 3 and link it to apoptosis. Compound **1** was similar to doxorubicin and caused a significant elevation (~7 fold) in the activity of active caspase 3 compared to untreated cells. Derivative **2e** caused an insignificant increase in the enzyme activity. These results correlate well with those reported in Table 3. This suggests that compound **1** induces apoptosis through caspase 3 while derivative **2e** works through a different pathway (Fig. 4).

2.2.5 Molecular docking. Molecular docking of the two most active synthesized compounds in inhibiting the activities of topoisomerase and p38 kinase (**1** and **2e**) to the active site in the crystal structures of both Pim-1 kinase (PDB ID: 5xyy) and DNA-topoisomerase II (PDB ID: 4EM7) enzymes was performed to investigate their binding interactions and to explore their binding modes. Moreover, doxorubicin and etoposide (ligands) were also docked against Topo II and Pim-1 kinase, respectively, in order to predict the proposed binding mode, affinity and the preferred orientation of each docking pose. Pim-1 kinase (PIM1), like MAPK, is a serine/threonine kinase. It is also a proto-oncogene implicated in many types of malignancies.[48] It is also responsible for cell proliferation, progression of cell cycle from G1 to S phase and from G2 to M phase. Selective inhibitors of MAPK and PIM1 are under clinical investigation as antitumor agents.[49,50] The results of docking study were reported as Topo II and PIM1 binding free energy (ΔG). The spontaneity of bindings was confirmed by the negative values of free energies (Table 4).

The interaction of etoposide with PIM1 (Fig. 5A) illustrates three hydrogen bonding interactions between important amino acid residues of the active site: Asp112, Thr106 and Met109. Additionally, it shows a good interaction CDOCKER score

(-6.61 kcal mol^{-1}). The proposed binding mode of compound **1** with PIM1 showed an affinity value of -5.69 kcal mol^{-1} (Table 4). The interaction demonstrated two hydrogen bond interactions; one between the S atom of the phthalazinonethione moiety and Met109, and a second between the nitrogen atom of position 1 of the phthalazinone moiety and Asp 168. The aromatic moiety was also involved in aromatic stacking interactions with Ile84 (Fig. 5B). Scrutinizing the binding pattern between derivative **2e** and PIM1 showed an affinity value of -5.93 kcal mol^{-1} (Table 4). Several interactions with the protein were observed including the formation of three hydrophobic interactions with the sulfur atom on the phthalazinone moiety and Thr106, Met109 and Lys53. Moreover, the phthalazinone moiety was involved in aromatic stacking interactions with Val38 and Leu108 (Fig. 5C).

The interaction of the ligand with DNA-topoisomerase II illustrated three hydrogen bonds between important amino acid residues of the active site, one with Asp78 and a second with Arg140 with an interaction CDOCKER score -6.44 kcal mol^{-1} (Table 4 and Fig. 6A). The proposed binding mode of compound **1** showed an affinity value of -6.06 kcal mol^{-1}. It showed two hydrogen bond interactions; the first between the sulphur atom of the phthalazinone moiety and Asn51 and the second between the nitrogen atom and the amino acid Asp78, in addition to two π bonds with Met83 (Fig. 6B). The binding interaction of derivative **2e** showed an affinity value of -6.04 kcal mol^{-1} with one hydrogen bonding interaction between the oxygen atom of the phthalazinone moiety atom and Ser124 (Fig. 6C).

The results of the docking study with PIM-1 kinase and Topo II are in good agreement with the inhibition profile of derivatives **1** and **2e** on MAPK and Topo II reported in this study.

2.2.6 Possible structure activity relationships (SAR). Compound **1** showed very strong anti-proliferative activity, due to the presence of NH and SH groups, which may interact with any unsaturated moiety in DNA or form hydrogen bonds with the nucleic bases of DNA, damaging them as indicated from its ability to induce caspase 3. For all the derivatives tested, those substituted with alkyl or acyl groups on the oxadiazole ring (compounds **2a–d**) displayed the least anti-proliferative activity. Examining the results in Table 2 pointed out that chloroacetyl derivative **2e** showed higher anti-proliferative activity than alkyl or acyl derivatives **2a–d**. The analysis of the results of the anti-proliferative activity showed that the disubstituted oxadiazol-phthalazinone derivatives (compounds **7a–g**) have higher anti-proliferative potency as compared to most monosubstituted oxadiazol-phthalazinone derivatives (compounds **2a–d**, **3** and **4a–d**). The substitution of OCH_3 or NO_2 groups at the *para* position of the attached benzene ring (compounds **7d** and **7e**) made them highly potent anti-proliferative compounds. These results were consistent with the published results[51] that showed that the presence of nitro or methoxy groups attached to benzene ring enhanced the anti-proliferative activity.

2.2.7 Conclusions. Seventeen oxadiazol-phthalazinone derivatives were synthesized under conventional and ultrasonic conditions along with the parent compound **1**. The ultrasonic methodology is easier, economical, faster, and environmentally benign. The ultrasonic approach proved to be extremely fast (4–10 min) providing better yields 85–94% as compared with the slower (50–85 min) conventional method in which the yield was 62–77%. Three oxadiazol-phthalazinone derivatives (**1**, **2e** and **7d**) exhibited significant and selective anti-proliferative activity against liver and breast cell lines without harming the normal fibroblasts. These derivatives acted through different molecular mechanisms and on multiple levels. They arrested the cell cycle progression and/or induced apoptosis. This has been manifested by the elevation in p53 and caspase 3, down-regulation of cdk1, and reduction in concentrations of MAPK and Topo II proteins. The latter results confirmed the molecular docking study. Compound **1** had the best profile on the gene and protein levels (arresting cell cycle and inducing apoptosis). The ability of derivatives **1** and **2e** to inhibit both MAPK and Topo II at submicromolar concentrations nominate these derivatives as potential candidates for further anticancer and antitumor studies.

3. Materials and methods

3.1. Chemistry

3.1.1 General. All melting points were taken on a Griffin and George melting-point apparatus and are uncorrected. IR spectra were recorded on Pye Unicam SP1200 spectrophotometer using the KBr wafer technique. ^{1}H NMR spectra were determined on a Varian Gemini 300 MHz and 400 MHz on Bruker Avance III using tetramethylsilane as an internal standard (chemical shifts in δ scale), while ^{13}C NMR spectra were run at 100 MHz. TMS was used as an internal standard in deuterated dimethylsulphoxide (DMSO-d_6). Chemical shifts were quoted as δ. Elemental analyses were carried out at the Microanalytical Unit, Faculty of Science, Ain Shams University, using a PerkinElmer 2400 CHN elemental analyzer, and satisfactory analytical data ($\pm$0.4) were obtained for all compounds. The purity of the synthesized compounds was controlled by thin layer chromatography (TLC) using aluminum sheet silica gel F_{254} (Merck). The ultrasound-assisted reactions were performed in Digital Ultrasonic Cleaner CD-4830 (35 KHz, 310 W). Compound **1** was synthesized as previously reported in the literature.[34]

3.1.2 General procedure for synthesis of 4-(5-(substituted thio)-1,3,4-oxadiazol-2-yl)phthalazin-1(2*H*)-one (2a–e)

Method A: ultrasonic conditions. A mixture of compound **1** (10 mmol) and alkyl or acyl halides, namely, ethyl iodide, benzyl chloride, phenacyl bromide, *m*-nitrophenacyl bromide and chloroacetyl chloride (10 mmol) in ethanol (20 mL) and catalytic amount of triethylamine (0.5 mL) was placed in an Erlenmeyer flask (50 mL) and subjected to ultrasound waves at room temperature for 5–10 min (controlled by TLC). The precipitated solid was filtered off, dried, and recrystallized from the appropriate solvent to afford the pure products **2a–e**.

Method B: conventional conditions. A mixture of compound **1** (10 mmol) and alkyl halides or acyl halides, namely, ethyl iodide, benzyl chloride, phenacyl bromide, *m*-nitrophenacyl bromide and chloroacetyl chloride (10 mmol) in ethanol (20 mL) and a catalytic amount of triethylamine (0.5 mL) was

heated under reflux for 50–65 min. The precipitated solid was filtered off, dried, and recrystallized from the appropriate solvent. All structures were confirmed by spectral data.

*4-(5-(Ethylthio)-1,3,4-oxadiazol-2-yl)phthalazin-1(2H)-one (**2a**).* Pale yellow crystals (92, 70%), mp 262–264 °C (dioxane). IR (ν/cm^{-1}): 3214, 3158 (NH), 3002 (CH aromatic), 2937, 2895 (CH aliphatic), 1667 (C=O). ^{1}H NMR (400 MHz, DMSO-d_6) δ (ppm): 1.43 (t, 3H, CH_2CH_3), 3.33 (q, 2H, CH_2CH_3), 7.91–8.06 (m, 2H, Ar–$H_{phthalazinone}$), 8.32 (d, 1H, Ar–$H_{phthalazinone}$, J = 8 Hz), 8.94 (d, 1H, Ar–$H_{phthalazinone}$, J = 8.4 Hz), 13.34 (br.s, 1H, NH, exchangeable with D_2O). Anal. calcd for $C_{12}H_{10}N_4O_2S$ (274.30): C, 52.55; H, 3.67; N, 20.43. Found C, 52.46; H, 3.71; N, 20.51.

*4-(5-(Benzylthio)-1,3,4-oxadiazol-2-yl)phthalazin-1(2H)-one (**2b**).* White crystals (90, 71%), mp 224–226 °C (ethanol/dioxane). IR (ν/cm^{-1}): 3223, 3167 (NH), 3051 (CH aromatic), 2925, 2894 (CH aliphatic), 1668 (C=O). ^{1}H NMR (400 MHz, DMSO-d_6) δ (ppm): 4.60 (s, 2H, SCH_2), 7.25–7.50 (m, 5H, Ar–$H_{C_6H_5}$), 7.91–7.95 (dd, 1H, Ar–$H_{phthalazinone}$, J = 8.4 Hz), 8.02–8.06 (dd, 1H, Ar–$H_{phthalazinone}$, J = 7.9 Hz), 8.33 (d, 1H, Ar–$H_{phthalazinone}$, J = 8 Hz), 8.91 (d, 1H, Ar–$H_{phthalazinone}$, J = 8 Hz), 13.41 (br.s, 1H, NH, exchangeable with D_2O). Anal. calcd for $C_{17}H_{12}N_4O_2S$ (336.37): C, 60.70; H, 3.60; N, 16.66. Found: C, 60.59; H, 3.54; N, 16.73.

*4-(5-((2-Oxo-2-phenylethyl)thio)-1,3,4-oxadiazol-2-yl)phthalazin-1(2H)-one (**2c**).* White crystals (87, 67%), mp 260–262 °C (dioxane). IR (ν/cm^{-1}): 3247, 3201 (NH), 3063 (CH aromatic), 2976 (CH aliphatic), 1680, 1675 (2C=O). ^{1}H NMR (300 MHz, DMSO-d_6) δ (ppm): 5.20 (s, 2H, SCH_2), 7.56–7.60 (m, 2H, Ar–$H_{C_6H_5}$), 7.69–7.72 (m, 1H, Ar–$H_{phthalazinone}$), 7.91–8.07 (m, 3H, Ar–$H_{C_6H_5}$ + 1H, Ar–$H_{phthalazinone}$), 8.32 (d, 1H, Ar–$H_{phthalazinone}$, J = 8 Hz), 8.88 (d, 1H, Ar–$H_{phthalazinone}$, J = 8 Hz), 13.36 (br.s, 1H, NH, exchangeable with D_2O). ^{13}C NMR (100 MHz, DMSO-d_6) δ (ppm): 41.1, 126.6 (2), 127.4, 127.8, 128.9 (2), 129.4 (2), 130.8, 132.8, 134.5, 134.8, 135.4, 159.6, 162.3, 164.7, 192.9. Anal. calcd for $C_{18}H_{12}N_4O_3S$ (364.38): C, 59.33; H, 3.32; N, 15.38. Found: C, 59.47; H, 3.40; N, 15.29.

*4-(5-((2-(3-Nitrophenyl)-2-oxoethyl)thio)-1,3,4-oxadiazol-2-yl) phthalazin-1(2H)-one (**2d**).* White crystals (85, 62%), mp 276–278 °C (dioxane). IR (ν/cm^{-1}), 3210 (NH), 3056 (CH aromatic), 2966, 2938 (CH aliphatic), 1687, 1676 (2C=O). ^{1}H NMR (300 MHz, DMSO-d_6) δ (ppm): 5.28 (s, 2H, SCH_2), 7.86–7.94 (m, 2H, Ar–H), 8.00–8.04 (m, 1H, Ar–$H_{phthalazinone}$), 8.31 (d, 1H, Ar–$H_{phthalazinone}$, J = 8 Hz), 8.47–8.53 (m, 2H, Ar–H Ar–$H_{phthalazinone}$), 8.74 (s, 1H, Ar–$H_{C_6H_4NO_2}$), 8.87 (d, 1H, Ar–$H_{phthalazinone}$, J = 8 Hz), 13.36 (br.s, 1H, NH, exchangeable with D_2O). ^{13}C NMR (100 MHz, DMSO-d_6) δ (ppm): 41.0, 123.2, 126.5, 126.6, 127.3, 127.8, 128.5, 130.8, 131.2, 132.8, 134.8, 135.0, 136.7, 148.5, 159.6, 162.4 (2), 191.8. Anal. calcd for $C_{18}H_{11}N_5O_5S$ (409.38): C, 52.81; H, 2.71; N, 17.11. Found: C, 52.99; H, 2.80; N, 17.22.

*S-(5-(4-Oxo-3,4-dihydrophthalazin-1-yl)-1,3,4-oxadiazol-2-yl)2-chloroethanethioate (**2e**).* Pale yellow crystals (86, 66%), mp 260–262 °C (dioxane). IR (ν/cm^{-1}): 3161 (NH), 3066 (CH aromatic), 2940, 2894 (CH aliphatic), 1688 (C=O). ^{1}H NMR (400 MHz, DMSO-d_6) δ (ppm): 3.54 (s, 2H, $COCH_2$), 7.91–7.95 (m, 1H, Ar–$H_{phthalazinone}$), 8.01–8.05 (m, 1H, Ar–$H_{phthalazinone}$), 8.32 (d, 1H, Ar–$H_{phthalazinone}$, J = 7.6 Hz), 8.69 (d, 1H, Ar–$H_{phthalazinone}$, J = 8 Hz), 13.39 (br.s, 1H, NH, exchangeable with D_2O). Anal. calcd for $C_{12}H_7ClN_4O_3S$ (322.72): C, 44.66; H, 2.19; N, 17.36. Found: C, 44.84; H, 2.22; N, 17.45.

3.1.3 Synthesis of *N′*-(5-(4-oxo-3,4-dihydrophthalazin-1-yl)-1,3,4-oxadiazol-2-yl)isonicotinohydrazide (3)

Method A: ultrasonic conditions. A mixture of compound **2e** (10 mmol) and isonicotinohydrazide (10 mmol) in dioxane (20 mL) was placed in an Erlenmeyer flask (50 mL) and subjected to ultrasound waves at room temperature for 8 min (controlled by TLC). The precipitated solid was filtered off, dried, and recrystallized from the appropriate solvent to afford the pure product **3**.

Method B: conventional conditions. A mixture of compound **2e** (10 mmol) and isonicotinohydrazide (10 mmol) in dioxane (20 mL) was heated under reflux for 55 min. The precipitated solid was filtered off, dried, and recrystallized from dioxane giving orange crystals of compound **3**.

*S-(5-(4-Oxo-3,4-dihydrophthalazin-1-yl)-1,3,4-oxadiazol-2-yl)2-(2-isonicotinoylhydrazinyl)ethanethioate (**3**).* Orange crystals (93, 75%), mp > 300 °C (dioxane). IR (ν/cm^{-1}): 3430, 3176 (NH), 3070 (CH aromatic), 2937, 2890 (CH aliphatic), 1724, 1663 (C=O). ^{1}H NMR (300 MHz, DMSO-d_6) δ (ppm): 4.03 (s, 2H, SCH_2), 7.84–8.94 (m, 8H, Ar–H + 2H, NH, exchangeable with D_2O), 13.00 (br.s, 1H, NH, exchangeable with D_2O). ^{13}C NMR (100 MHz, DMSO-d_6) δ (ppm): 46.0, 121.9, 126.1, 126.3, 126.5, 126.6, 127.4, 127.8, 131.0, 132.4, 132.6, 132.7, 134.5, 134.7, 159.6, 161.7, 166.3, 169.2. Anal. calcd for $C_{18}H_{13}N_7O_4S$ (423.4): C, 51.06; H, 3.09; N, 23.16. Found: C, 52.22; H, 3.18; N, 23.26.

3.1.4 General procedure for synthesis of 2-((5-(4-oxo-3,4-dihydrophthalazin-1-yl)-1,3,4-oxadiazol-2-yl)thio)acetamide derivatives (4a–d)

Method A: ultrasonic conditions. A mixture of compound **1** (10 mmol) and 2-chloro-*N*-phenylacetamide derivatives (10 mmol) in dioxane (20 mL) was placed in an Erlenmeyer flask (50 mL) and subjected to ultrasound waves at room temperature for 10 min (controlled by TLC). The precipitated solid was filtered off, dried, and recrystallized from the appropriate solvent to afford the pure products **4a–d**.

Method B: conventional conditions. A mixture of compound **1** (10 mmol), and 2-chloro-*N*-phenylacetamide derivatives (10 mmol) in dioxane (20 mL) was heated under reflux for 65–75 min. The precipitated solid was filtered off, dried, and recrystallized from the appropriate solvent. All structures were confirmed by spectral data as discussed below.

*N-(4-Acetylphenyl)-2-((5-(4-oxo-3,4-dihydrophthalazin-1-yl)-1,3,4-oxadiazol-2-yl)thio)acetamide (**4a**).* White crystals (92, 73%), mp > 300 °C (dioxane). IR (ν/cm^{-1}): 3322, 3215 (NH), 3045 (CH aromatic), 2969, 2895 (CH aliphatic), 1691, 1668 (2C=O). ^{1}H NMR (300 MHz, DMSO-d_6) δ (ppm): 2.49 (s, 3H, $COCH_3$), 4.44 (s, 2H, SCH_2), 7.70 (d, 2H, Ar–$H_{C_6H_4OCH_3}$, J = 8.4 Hz), 7.92–7.95 (m, 2H, Ar–H + 1H, Ar–$H_{phthalazinone}$), 8.00–8.03 (m, 1H, Ar–$H_{phthalazinone}$), 8.31 (d, 1H, Ar–$H_{phthalazinone}$, J = 8 Hz), 8.90 (d, 1H, Ar–$H_{phthalazinone}$, J = 8 Hz), 10.78 (br.s, 1H, NH, exchangeable with D_2O), 13.37 (br.s, 1H, NH, exchangeable with D_2O). ^{13}C NMR (100 MHz, DMSO-d_6) δ (ppm): 26.6, 37.4, 118.9 (2), 126.6 (2), 127.4, 127.8, 130.0 (2), 130.8, 132.5, 132.8, 134.8, 143.3, 159.6, 162.3, 164.7, 165.7, 196.9. Anal. calcd for

$C_{20}H_{15}N_5O_4S$ (421.43): C, 57.00; H, 3.59; N, 16.62. Found: C, 57.22; H, 3.64; N, 16.71.

*2-((5-(4-Oxo-3,4-dihydrophthalazin-1-yl)-1,3,4-oxadiazol-2-yl) thio)-N-(4-sulfamoylphenyl)acetamide (**4b**).* White crystals (94, 77%), mp > 300 °C (dioxane). IR (ν/cm^{-1}): 3311, 3268, 3163 (NH, NH_2), 3065 (CH aromatic), 2934, 2895 (CH aliphatic), 1691, 1663 (2C=O). ^{1}H NMR (300 MHz, DMSO-d_6) δ (ppm): 4.43 (s, 2H, SCH_2), 7.25 (br.s, 2H, NH_2, exchangeable with D_2O), 7.71–7.78 (m, 4H, Ar–H), 7.91–8.05 (m, 2H, Ar–$H_{phthalazinone}$), 8.32 (d, 1H, Ar–$H_{phthalazinone}$, J = 8.8 Hz), 8.90 (d, 1H, Ar–$H_{phthalazinone}$, J = 8 Hz), 10.79 (br.s, 1H, NH, exchangeable with D_2O), 13.37 (br.s, 1H, NH, exchangeable with D_2O). ^{13}C NMR (400 MHz, DMSO-d_6) δ (ppm): 37.4, 119.2 (2), 126.6, 127.2, 127.4 (3), 127.8, 130.8, 132.8, 134.8, 139.2, 141.9, 159.6, 162.3, 164.7, 165.7. Anal. calcd for $C_{18}H_{14}N_6O_5S_2$ (485.47): C, 47.16; H, 3.08; N, 18.33. Found: C, 47.33; H, 3.18; N, 18.44.

*2-((5-(4-Oxo-3,4-dihydrophthalazin-1-yl)-1,3,4-oxadiazol-2-yl) thio)-N-(p-tolyl)acetamide (**4c**).* Grey crystals (90, 74%), mp 265–267 °C (dioxane). IR (ν/cm^{-1}): 3308, 3215 (NH), 3074 (CH aromatic), 2934, 2894 (CH aliphatic), 1689, 1657 (2C=O). ^{1}H NMR (300 MHz, DMSO-d_6) δ (ppm): 2.29 (s, 3H, CH_3), 4.40 (s, 2H, SCH_2), 7.01 (d, 2H, Ar–H, J = 8.4 Hz), 7.46 (d, 2H, Ar–H, J = 8.4 Hz), 7.89–8.04 (m, 2H, Ar–$H_{phthalazinone}$), 8.31 (d, 1H, Ar–$H_{phthalazinone}$, J = 8.1 Hz), 8.90 (d, 1H, Ar–$H_{phthalazinone}$, J = 8.1 Hz), 10.41 (br.s, 1H, NH, exchangeable with D_2O), 13.36 (br.s, 1H, NH, exchangeable with D_2O). Anal. calcd for $C_{19}H_{15}N_5O_3S$ (393.42): C, 58.01; H, 3.84; N, 17.80. Found C, 58.19; H, 3.92; N, 17.91.

*N-(4-Chlorophenyl)-2-((5-(4-oxo-3,4-dihydrophthalazin-1-yl)-1,3,4-oxadiazol-2-yl)thio)acetamide (**4d**).* White crystals (91, 70%), mp 206–208 °C (ethanol). IR (ν/cm^{-1}): 3305, 3163 (NH), 3044 (CH aromatic), 2978, 2941 (CH aliphatic), 1691, 1657 (2C=O). ^{1}H NMR (300 MHz, DMSO-d_6) δ (ppm): 4.40 (s, 2H, SCH_2), 7.35–7.38 (dd, 2H, Ar–$H_{C_6H_4Cl}$, J = 8 Hz), 7.60–7.63 (d, 2H, Ar–$H_{C_6H_4Cl}$, J = 8 Hz), 7.92–8.05 (m, 2H, Ar–$H_{phthalazinone}$), 8.32 (d, 1H, Ar–$H_{phthalazinone}$, J = 8 Hz), 8.91 (d, 1H, Ar–$H_{phthalazinone}$, J = 8 Hz), 10.76 (br.s, 1H, NH, exchangeable with D_2O), 13.42 (br.s, 1H, NH, exchangeable with D_2O). ^{13}C NMR (100 MHz, DMSO-d_6) δ (ppm): 37.3, 121.1, 121.2, 126.6, 127.4 (2), 127.8 (2), 129.2, 130.9, 131.8, 134.8 (2), 138.0, 159.6, 162.3, 164.7, 165.3. Anal. calcd for $C_{18}H_{12}ClN_5O_3S$ (413.84): C, 52.24; H, 2.92; N, 16.92. Found: C, 52.16; H, 2.83; N, 17.09.

3.1.5 General procedure for synthesis of 4-(1,3,4-oxadiazol-2-yl)phthalazin-1(2*H*)-one derivatives (7a–g)

Method A: ultrasonic conditions. A mixture of compound **1** (10 mmol), formaldehyde (20 mmol) and primary amines namely, *p*-toluidine, *p*-chloroaniline, *o*-chloroaniline, *p*-anisidine, *p*-nitroaniline, 3-aminopyridine and cyclohexyl amine (20 mmol) in dioxane (20 mL) were placed in an Erlenmeyer flask (50 mL) and subjected to ultrasound waves at room temperature for 5–10 min (controlled by TLC). The precipitated solid was filtered off, dried, and recrystallized from the appropriate solvent to afford the pure products **7a–g**.

Method B: conventional conditions. A mixture of compound **1** (10 mmol), formaldehyde (20 mmol) and primary amines (20 mmol) (Table 1) in dioxane (20 mL) was stirred at room temperature for 72–83 min. The precipitated solid was filtered off, dried, and recrystallized from the appropriate solvent.

*2-((p-Tolylamino)methyl)-4-(5-(((p-tolylamino)methyl)thio)-1,3,4-oxadiazol-2-yl)phthalazin-1(2H)-one (**7a**).* Buff crystals (94, 68%), mp 175–177 °C (ethanol). IR (ν/cm^{-1}): 3180 (NH), 3078 (CH aromatic), 2920, 2892 (CH aliphatic), 1669 (C=O). ^{1}H NMR (300 MHz, DMSO-d_6) δ (ppm): 2.28 (s, 3H, CH_3), 2.50 (s, 3H, CH_3), 5.42–5.52 (dd, 2H, SCH_2N, J = 9 Hz), 5.90–6.08 (dd, 2H, NCH_2N, J = 9 Hz), 6.45–7.80 (m, 4H, Ar–H), 7.92–8.05 (m, 4H, Ar–H), 8.31–8.34 (m, 2H, Ar–$H_{phthalazinone}$), 8.66–8.71 (m, 2H, Ar–$H_{phthalazinone}$), 13.38–13.44 (m, 2H, 2NH, exchangeable with D_2O). Calcd for $C_{26}H_{24}N_6O_2S$ (484.6): C, 64.44; H, 4.99; N, 17.34. Found: C, 64.25; H, 4.89; N, 17.27.

*2-(((4-Chlorophenyl)amino)methyl)-4-(5-((((4-chlorophenyl) amino)methyl)thio)-1,3,4-oxadiazol-2-yl)phthalazin-1(2H)-one (**7b**).* Buff crystals (93, 76%), mp 138–140 °C (ethanol). IR (ν/cm^{-1}): 3356 (NH), 3079 (CH aromatic), 2961, 2889 (CH aliphatic), 1667 (C=O). ^{1}H NMR (300 MHz, DMSO-d_6) δ (ppm): ^{1}H NMR (300 MHz, DMSO-d_6) δ (ppm): 5.39–5.48 (dd, 2H, SCH_2N, J = 16 Hz), 5.50–5.77 (dd, 2H, NCH_2N, J = 16 Hz), 6.62–7.69 (m, 8H, Ar–H), 7.85–8.74 (m, 4H, Ar–$H_{phthalazinone}$), 13.00–13.45 (m, 2H, 2NH, exchangeable with D_2O). ^{13}C NMR (400 MHz, DMSO-d_6) δ (ppm): 57.8, 73.9, 113.6 (2), 115.6, 119.6 (2), 120.8, 125.8, 127.04, 127.5, 128.4, 128.6, 130.1, 132.9, 133.2, 133.3, 134.6, 141.7 (2), 155.3, 158.2, 159.8, 175.7. Anal. calcd for $C_{24}H_{18}Cl_2N_6O_2S$ (525.4): C, 54.86; H, 3.45; N, 16.00. Found: C, 54.67; H, 3.35; N, 16.11.

*2-(((2-Chlorophenyl)amino)methyl)-4-(5-((((2-chlorophenyl) amino)methyl)thio)-1,3,4-oxadiazol-2-yl)phthalazin-1(2H)-one (**7c**).* White crystals (90, 74%), mp 240–242 °C (ethanol). IR (ν/cm^{-1}): 3171, 3111 (NH), 3071 (CH aromatic), 2956, 2893 (CH aliphatic), 1669 (C=O). ^{1}H NMR (300 MHz, DMSO-d_6) δ (ppm): 5.51–5.81 (dd, 2H, SCH_2N, J = 11.6 Hz), 5.90–5.99 (dd, 2H, NCH_2N, J = 11.6 Hz), 6.16–7.92 (m, 8H, Ar–H), 7.94–8.41 (m, 4H, Ar–$H_{phthalazinone}$), 13.00–13.48 (m, 2H, 2NH exchangeable with D_2O). Anal. calcd for $C_{24}H_{18}Cl_2N_6O_2S$ (525.4): C, 54.86; H, 3.45; N, 16.00. Found: C, 54.65; H, 3.37; N, 15.90.

*2-(((4-Methoxyphenyl)amino)methyl)-4-(5-((((4-methoxyphenyl) amino)methyl)thio)-1,3,4-oxadiazol-2-yl)phthalazin-1(2H)-one (**7d**).* Brown crystals (91, 67%), mp 158–161 °C (ethanol). IR (ν/cm^{-1}): 3203 (NH), 3074 (CH aromatic), 2955 (CH aliphatic), 1666 (C=O). ^{1}H NMR (300 MHz, DMSO-d_6) δ (ppm): 3.73 (s, 3H, OCH_3), 3.79 (s, 3H, OCH_3), 5.51–5.89 (dd, 2H, SCH_2N, J = 12 Hz), 5.75–5.89 (dd, 2H, NCH_2N, J = 10.4 Hz), 6.68–6.95 (m, 4H, Ar–H), 7.04–7.37 (m, 4H, Ar–H), 7.43–8.75 (m, 4H, Ar–$H_{phthalazinone}$), 12.99–13.40 (m, 2H, 2-NH, exchangeable with D_2O). Anal. calcd for $C_{26}H_{24}N_6O_4S$ (516.6): C, 60.45; H, 4.68; N, 16.27. Found: C, 60.23; H, 4.57; N, 16.19.

*2-(((4-Nitrophenyl)amino)methyl)-4-(5-((((4-nitrophenyl)amino) methyl)thio)-1,3,4-oxadiazol-2-yl)phthalazin-1(2H)-one (**7e**).* Yellow crystals (92, 77%), mp 213–215 °C (ethanol/dioxane). IR (ν/cm^{-1}): 3393 (NH), 3079 (CH aromatic), 2924, 2895 (CH aliphatic), 1671 (C=O). ^{1}H NMR (300 MHz, DMSO-d_6) δ (ppm): 5.50–5.52 (dd, 2H, SCH_2N, J = 6.9 Hz), 5.68–5.70 (dd, 2H, NCH_2N, J = 6.9 Hz), 6.78–6.80 (d, 2H, Ar–$H_{nitrophenyl}$, J = 6 Hz), 7.07–7.10 (d, 2H, Ar–$H_{nitrophenyl}$, J = 6 Hz), 7.84–8.61 (m, 8H, Ar–H), 13.41–13.42 (m, 2H, 2NH exchangeable with D_2O). Anal.

calcd for $C_{24}H_{18}N_8O_6S$ (546.5): C, 52.75; H, 3.32; N, 20.50. Found: C, 52.56; H, 3.24; N, 20.38.

*2-((Pyridin-3-ylamino)methyl)-4-(5-(((pyridin-3-ylamino)methyl) thio)-1,3,4-oxadiazol-2-yl)phthalazin-1(2H)-one (**7f**).* White crystals (88, 69%), mp 190–192 °C (ethanol). IR (ν/cm^{-1}): 3395 (NH), 3085 (CH aromatic), 2925 (CH aliphatic), 1691 (C=O), 1650 (C=N). ^{1}H NMR (400 MHz, DMSO-d_6) δ (ppm): 4.57–5.08 (m, 1H, NH, exchangeable with D_2O), 5.12–5.49 (m, 1H, NH, exchangeable with D_2O), 5.49–5.65 (dd, 2H, SCH_2N, $J = 12$ Hz), 5.75–5.82 (dd, 2H, NCH_2N, $J = 12$ Hz), 7.08–7.50 (m, 4H, Ar–$H_{pyridyl}$), 7.78–7.96 (m, 4H, Ar–$H_{pyridyl}$), 8.18–8.34 (m, 2H, Ar–$H_{phthalazinone}$), 8.49 (d, 1H, Ar–$H_{phthalazinone}$, J = 8.4 Hz), 8.59 (d, 1H, Ar–$H_{phthalazinone}$, J = 8.4 Hz). ^{13}C NMR (400 MHz, DMSO-d_6) δ (ppm): 59.3, 82.3, 119.3 (2), 120.8, 124.1, 126.2 (2), 126.8 (2), 127.6, 127.7, 132.7 (2), 134.5 (2), 136.1, 138.7, 143.1 (2), 159.1, 164.9. Anal. calcd for $C_{22}H_{18}N_8O_2S$ (458.50): C, 57.63; H, 3.96; N, 24.44. Found C, 57.79; H, 4.01; N, 24.52.

*4-(5-(((Cyclohexylamino)methyl)thio)-1,3,4-oxadiazol-2-yl) phthalazin-1(2H)-one (**7g**).* Pale yellow crystals (95, 75%), mp 240–242 °C (ethanol/dioxane). IR (ν/cm^{-1}): 3306 (NH), 3112 (CH aromatic), 2971, 2894 (CH aliphatic), 1672 (C=O). ^{1}H NMR (300 MHz, DMSO-d_6) δ (ppm): 1.18–1.85 (m, 11$H_{cyclohexyl}$), 5.38–5.48 (dd, 2H, CH–$N_{cyclohexyl}$), 7.86–8.06 (m, 2H, Ar–$H_{phthalazinone}$), 8.25–8.74 (m, 2H, Ar–$H_{phthalazinone}$), 12.99–13.04 (m, 2H, 2NH, exchangeable with D_2O). Anal. calcd for $C_{17}H_{19}N_5O_2S$ (357.4): C, 57.13; H, 5.36; N, 19.59. Found C, 56.98; H, 5.27; N, 19.48.

3.2. Biology

3.2.1 Anti-proliferative (cytotoxic) activity (MTT assay). The anti-proliferative activity of the novel compounds against the growth of human cancer epithelial cell lines; liver (HepG2, passage # 11) and breast (MCF7, passage # 13), in addition to normal fibroblasts (WI-38) was assessed using the MTT assay as described elsewhere.[52] The cell lines, fetal bovine serum, media, and trypsin were obtained from the American Type Culture Collection (ATCC; Manassas, VA, USA). Briefly, 2×10^6 cells were seeded in every well, and the cells were treated with different concentrations (0.5, 1, 10, 20, 50, and 100 μM) of the novel derivatives and incubated for 48 h. After 48 h, 20 μL of MTT solution (5 mg mL^{-1}) was added and incubated for 4 h. The formazan formed in every well was dissolved in DMSO (100 μL), and the optical density was recorded at 570 nm. Control untreated cells in addition to doxorubicin treated cells were performed for comparison. The data are expressed as mean ± SEM for two independent experiments.

3.2.2 Assessment of the expression of p53, cdk1, caspase-3, and txnrd1 by qRT-PCR. The HepG2 cells were treated with the novel derivatives at the IC_{50} concentrations reported in Table 2 in DMSO for 8 h. Total RNA was isolated from the cells using TRIzol reagent from Sigma (St. Louis, MO, USA). Specific primers for p53, cdk1, caspase-3, txnrd1 and glyceraldehyde-3-phosphate dehydrogenase (GAPDH) as a house-keeping gene (Table 5), were used in reverse transcription (RT) and q-PCR. RT and q-PCR were executed as described previously[53] using Maxima SYBR Green qPCR Master Mix (Bioline, London, UK). Every sample ($n = 4$) was analyzed in triplicate. The ΔC_t (cycle threshold, C_t) method was used to determine the differences in gene expression between groups.[54] The changes were normalized against GAPDH of the same sample and expressed as fold change compared with the control untreated cells.

3.2.3 Inhibitory activity of novel derivatives on p38 mitogen-activated protein kinase (MAPK) and topoisomerase II (Topo II). The inhibitory effect of novel derivatives on MAPK and Topo II concentration was determined using Invitrogen (Carlsbad, CA, USA) kit (Catalog # KHO0061) and Mybiosource (San Diego, CA, USA), respectively based on sandwich ELISA methods.

3.2.4 Measurement of the active cleaved caspase 3 activity. The active cleaved caspase-3 activity was determined in HepG2 cells after incubation with the IC_{50} concentration of compound **1** and derivative **2e** for 12 h according to the method of Hasegawa *et al.*,[55] using a colorimetric assay kit provided from Abcam (UK).

3.2.5 Molecular docking. The molecular docking study was conducted in order to elucidate the interactions of the investigated compounds with the target enzymes: Pim-1 kinase and Topo II. First, the crystal structure of both Pim-1 kinase and Topo II co-crystallized with doxorubicin was retrieved from the Protein Data Bank: Pim-1 kinase (PDB ID: 5xyy) and DNA-topoisomerase II (ID: 2ggv). The docking study was performed using Accelrys software (MOE 2015.10) provided by the Computer Drug Design Lab in Pharmaceutical Chemistry Department, Faculty of Pharmacy, Ain Shams University. Protein preparation for docking study was performed following the standard protein preparation procedure integrated in Accelry's discovery studio 2.5. The 3D structures of doxorubicin and derivatives under investigation were refined using CHARMM force field with full potential. Docking simulations were run using CDOCKER protocol where maximum bad orientations were 800 and orientation vdW energy threshold was 300. Simulated annealing was then carried out, consisting of a heating phase 700 K with 2000 steps and a cooling phase back to 5000 steps. In order to assess the docking poses, the binding energy was calculated as a score. The top 10 docking poses were finally saved. Docking poses were ranked according to their CDOCKER interaction energy, and the top pose was chosen for analysis of interactions for each derivative.

3.3. Statistical analysis of data

Statistical analysis was performed using One Way ANOVA for comparing different groups. The distribution of data was first tested using the Kolmogorov–Sminrov test. Results were expressed as mean ± SEM. Paired comparisons between groups were performed using Tukey-HSD test. The confidence limit was set at 95% and the difference at $p < 0.05$ was considered significant.

Conflicts of interest

The authors declare no conflict of interest, financial or otherwise.

Acknowledgements

The authors sincerely acknowledge Dr Jeanette Roberts (Professor of Medicinal Chemistry and Dean Emerita, University of Wisconsin-Madison) for critically reading the manuscript.

References

1 I. H. Hall, B. J. Barnes, E. S. Ward, J. R. Wheaton, K. A. Shaffer, S. E. Cho and A. E. Warren, *Arch. Pharm.*, 2001, **334**, 229–234.
2 I. H. Hall, E. S. Hall and O. T. Wong, *Anti-Cancer Drugs*, 1992, **3**, 55–62.
3 I. H. Hall, D. W. Covington, J. R. Wheaton, R. A. Izydore and X. Zhou, *Pharmazie*, 2001, **56**, 168–174.
4 M. C. Cardia, S. Distinto, E. Maccioni, A. Plumitallo, L. Sanna, M. L. Sanna and S. Vigo, *J. Heterocycl. Chem.*, 2009, **46**, 674–679.
5 V. M. Loh, X.-l. Cockcroft, K. J. Dillon, L. Dixon, J. Drzewiecki, P. J. Eversley, S. Gomez, J. Hoare, F. Kerrigan, I. T. W. Matthews, K. A. Menear, N. M. B. Martin, R. F. Newton, J. Paul, G. C. M. Smith, J. Vilec and A. J. Whittlec, *Bioorg. Med. Chem. Lett.*, 2005, **15**, 2235–2238.
6 X. L. Cockcroft, K. J. Dillon, L. Dixon, J. Drzewiecki, F. Kerrigan, V. M. Loh, N. M. B. Martin, K. A. Menear and G. C. M. Smith, *Bioorg. Med. Chem. Lett.*, 2006, **16**, 1040–1044.
7 K. A. Menear, C. Adcock, R. Boulter, X. Cockcroft, L. Copsey, A. Cranston, K. J. Dillon, J. Drzewiecki, S. Garman, S. Gomez, H. Javaid, F. Kerrigan, C. Knights, A. Lau, V. M. Loh, I. T. W. Matthews, S. Moore, M. J. O'Connor, G. C. M. Smith and N. M. B. Martin, *J. Med. Chem.*, 2008, **51**, 6581–6591.
8 S. L. Gaonkar, K. M. L. Rai and B. Prabhuswamy, *Eur. J. Med. Chem.*, 2006, **41**, 841–846.
9 T. M. C. Tan, Y. Chen, K. H. Kong, J. Bai, Y. Li, S. G. Lim, T. H. Ang and Y. Lam, *Antiviral Res.*, 2006, **71**, 7–14.
10 Y. Li, J. Liu, H. Zhang, X. Yang and Z. Liu, *Bioorg. Med. Chem. Lett.*, 2006, **16**, 2278–2282.
11 A. S. Aborai, H. M. Abdel-Rahman, N. M. Mahfouz and M. A. Gendy, *Bioorg. Med. Chem.*, 2006, **14**, 1236–1246.
12 M. T. Khan, M. I. Choudhary, K. M. Khan, M. Rani and A. U. Rahman, *Bioorg. Med. Chem.*, 2005, **13**, 3385–3395.
13 C. Loetchutinat, F. Chau and S. Mankhetkorn, *Chem. Pharm. Bull.*, 2003, **51**, 728–730.
14 A. H. Abadi, A. A. H. Eissa and G. S. Hassan, *Chem. Pharm. Bull.*, 2003, **51**, 838–844.
15 B. G. Szczepankiewicz, G. Liu, H. S. Jae, A. S. Tasker, I. W. Gunawardana, T. W. v. Geldern, S. L. Gwaltney, J. R. Wu-Wong, L. Gehrke, W. J. Chiou, R. B. Credo, J. D. Alder, M. A. Nukkala, N. A. Zielinski, K. Jarvis, K. W. Mollison, D. J. Frost, J. L. Bauch, Y. H. Hui, A. K. Claiborne, Q. Li and S. H. Rosenberg, *J. Med. Chem.*, 2001, **44**, 4416–4430.
16 D. Kumar, S. Sundaree, E. O. Johnson and K. Shah, *Bioorg. Med. Chem. Lett.*, 2009, **19**, 4492–4494.
17 J. T. Palmer, B. L. Hirschbein, H. Cheung, J. McCarter, J. W. Janc, W. Z. Yu and G. Wesolowski, *Bioorg. Med. Chem. Lett.*, 2006, **16**, 2909–2914.
18 R. N. Warrener, *Eur. J. Org. Chem.*, 2000, 3363–3380.
19 M. Guan, Z. Q. Bian, Y. F. Zhou, F. Y. Li, Z. J. Li and C. H. Huang, *Chem. Commun.*, 2003, 2708–2709.
20 H. Lai, D. Dou, S. Aravapalli, T. Teramoto, G. H. Lushington, T. M. Mwania, K. R. Alliston, D. M. Eichhorn, R. Padmanabhan and W. C. Groutas, *Bioorg. Med. Chem.*, 2013, **21**, 102–113.
21 T. J. Mason and J. P. Lorimer, *J. Chem. Technol. Biotechnol.*, 2004, **79**, 207–208.
22 M. R. Shaaban, T. S. Saleh, F. H. Osman and A. M. Farag, *J. Heterocycl. Chem.*, 2007, **44**, 177–181.
23 S. Dandapani and L. A. Marcaurelle, *Curr. Opin. Chem. Biol.*, 2010, **14**, 362–370.
24 T. J. Mason and D. Peters, *Angew. Chem., Int. Ed.*, 2003, **42**, 2331–2335.
25 M. A. EL-Hashash, E. A. El-Bordany, M. I. Marzouk, A. M. El-Naggar, T. M. S. Nawar and W. M. El-Sayed, *Anti Cancer Agents Med. Chem.*, 2018, **18**, 1589–1598.
26 I. H. Eissa, A. M. El-Naggar and M. A. El-Hashash, *Bioorg. Chem.*, 2016, **67**, 43–56.
27 I. H. Eissaa, A. M. El-Naggar, N. E. A. Abd El-Sattar and A. S. A. Youssef, *Anti Cancer Agents Med. Chem.*, 2018, **18**, 195–209.
28 M. A. Ismail, A. Negm, R. K. Arafa, E. Abdel-Latif and W. M. El-Sayed, *Eur. J. Med. Chem.*, 2019, **169**, 76–88.
29 M. A. Ismail, M. M. Youssef, R. K. Arafa, S. S. Al-Shihry and W. M. El-Sayed, *Eur. J. Med. Chem.*, 2017, **126**, 789–798.
30 k. A. M. Abouzid, G. H. Al-Ansary and A. M. El-Naggar, *Eur. J. Med. Chem.*, 2017, **134**, 357–365.
31 A. M. El-Naggar, M. M. Hemdan and S. R. Atta-Allah, *J. Heterocycl. Chem.*, 2017, **54**, 3519.
32 A. M. El-Naggar, A. K. Khalil, H. M. Zeidan and W. M. El-Sayed, *Anti Cancer Agents Med. Chem.*, 2017, **17**, 1644–1651.
33 M. H. Hekal and F. S. M. Abu El-Azm, *J. Heterocycl. Chem.*, 2017, **54**, 3056–3064.
34 M. R. Mahmoud, W. S. I. Abou-Elmagd, H. A. Derbala and M. H. Hekal, *Chin. J. Chem.*, 2011, **29**, 1446–1450.
35 Y. Sun, P. Xia, H. Zhang, B. Liu and Y. Shi, *Am. J. Cancer Res.*, 2016, **6**, 114–125.
36 J. Herrero-Ruiz, M. Mora-Santos, S. Giráldez, C. Sáez, M. Á. Japón, M. Tortolero and F. Romero, *Oncotarget*, 2014, **5**, 7563–7574.
37 J. J. Liu, Q. Liu, H. L. Wei, J. Yi, H. S. Zhao and L. P. Gao, *Pharmazie*, 2011, **66**, 440–444.
38 T. Ozaki and A. Nakagawara, *Cancers*, 2011, **3**, 994–1013.
39 E. Senturk and J. J. Manfredi, *Methods Mol. Biol.*, 2013, **962**, 49–61.
40 M. Olsson and B. Zhivotovsky, *Cell Death Differ.*, 2011, **18**, 1441–1449.
41 J. M. Enserink and R. D. Kolodner, *Cell Div.*, 2010, **5**, 1–41.
42 E. S. Arnér and A. Holmgren, *Eur. J. Biochem.*, 2000, **267**, 6102–6109.
43 P. Nguyen, R. T. Awwad, D. D. Smart, D. R. Spitz and D. Gius, *Cancer Lett.*, 2006, **2361**, 64–74.

44 K. F. Tonissen and G. Di Trapani, *Mol. Nutr. Food Res.*, 2009, **53**, 87–103.
45 G. Ambrosini, H. S. Cheema, S. Seelman, E. B. Sambol, S. Singer and G. K. Schwartz, *Mol. Cancer Ther.*, 2008, **7**, 890–896.
46 J. L. Nitiss, *Nat. Rev. Cancer*, 2009, **9**, 327–337.
47 E. Willmore, S. de Caux and N. J. Sunter, *Blood*, 2004, **103**, 4659–4665.
48 X. Zhang, M. Song, J. K. Kundu, M. H. Lee and Z. Z. Liu, *Journal of Cancer Prevention*, 2018, **23**, 109–116.
49 B. T. Le, M. Kumarasiri, J. R. Adams, M. Yu, R. Milne, M. J. Sykes and S. Wang, *Future Med. Chem.*, 2015, **7**, 35–53.
50 Y. Tursynbay, J. Zhang, Z. Li, T. Tokay, Z. Zhumadilov, D. Wu and Y. Xie, *Biomed. Rep.*, 2016, **4**, 140–146.
51 I. Malík, J. Csöllei, J. Jampílek, L. Stanzel, I. Zadražilová, J. Hošek, Š. Pospíšilová, A. Čížek, A. Coffey and J. O' Mahony, *Molecules*, 2016, **21**, 1274.
52 P. Skehan, R. Storeng, D. Scudiero, A. Monks, J. McMahon, D. Vistica, J. T. Warren, H. Bokesch, S. Kenney and M. R. Boyd, *J. Natl. Cancer Inst.*, 1990, **82**, 1107–1112.
53 R. A. Hussein, E. A. El-Husseiny, L. A. Hassanin and W. M. El-Sayed, *Int. J. Clin. Pharmacol. Toxicol.*, 2017, **6**, 270–279.
54 S. A. El-Metwally, A. K. Khalil, A. M. El-Naggar and W. M. El-Sayed, *Anti-Cancer Agents Med. Chem.*, 2018, **18**, 1761–1769.
55 S. Kamada, M. Washida, J. I. Hasegawa, H. Kusano, Y. Funahashi and Y. Tsujimoto, *Oncogene*, 1997, **15**, 285–290.

